Journal of Computational Electronics (2022) 21:814–825
https://doi.org/10.1007/s10825-022-01905-w

FEM simulation and material selection for enhancing the performance of a RF-MEMS capacitive switch

Raj Kumari[1] · **Mahesh Angira**[1]

Received: 22 December 2021 / Accepted: 7 May 2022 / Published online: 10 June 2022

Abstract
The performance of radio-frequency microelectromechanical systems (RF-MEMS) is based on the material and geometry of the switching device. The first step of any design process is material selection. Thus, this work is directed towards selecting the best materials for the actuating layer and dielectric of RF-MEMS capacitive switches. Material selection is aimed at increasing the switching speed and power handling of the MEMS switch. TOPSIS (Technique for Order of Preference by Similarity to Ideal Solution) and VIKOR (Vlsekriterijumska Optimizacija Kompromisno Resenje) decision-making techniques are utilized to select suitable materials for the structural and dielectric layers. The material indices for selecting the optimum dielectric are relative permittivity, resistivity, thermal conductivity, Young's modulus (YM) and thermal expansion coefficient (TEC). For the structural layer, the YM, thermal conductivity, TEC, melting point (MP) and density-to-YM ratio are selected as material indices. Results obtained from TOPSIS and VIKOR are validated by simulating the electromagnetic and electromechanical characteristics of the shunt RF-MEMS capacitive switch. Investigation and validation results show that graphite and Al_2O_3 are the best materials for the switch structure and dielectric, respectively, to ensure high switching speed, with a pull-in time of 15.2 µs, release time 6.53 µs and high potential for power handling, with self-actuation power of 27.1 W. The simulated switch is found suitable for X and Ku band applications, offering insertion loss of less than −0.7 dB and isolation greater than −20 dB.

Keywords Dielectric · FEM · MADM · Pull-in voltage · RF-MEMS · Switching speed

1 Introduction

Today, radio-frequency microelectromechanical systems (RF-MEMS) are at the cutting edge of technology, as they offer wideband operation with good RF performance. These devices find wide application in RF components and systems design, wireless sensor networks, biomedical fields, defense and satellite communication [1]. Devices based on RF-MEMS technology can extend their performance and productivity by using MEMS components in the design. MEMS devices have the unique ability to perform both mechanical and electrical operations. Among various MEMS devices, the RF-MEMS switch is the basic component employed in almost all wireless communication systems. RF-MEMS switches have replaced nearly all the existing common switches such as PIN diodes, field-effect transistors (FET) and tunnel field-effect transistors (TFETs) due to their unique electromechanical functionality [2, 3]. Solid-state switches consume more power, while RF-MEMS switches show outstanding RF performance and low power consumption, along with their small size. However, RF-MEMS switches suffer from lack of reliability, high power handling capability and switching speed [4]. Much research has been conducted to deal with these issues, and studies suggest that these can be remarkably improved. To improve switching speed and RF power handling with better electromagnetic and electromechanical performance of switches, careful selection of the material for different components is critical. Different material selection methodologies have been developed where suitable material properties for the desired performance are derived to select the best material out of a pool of materials. TOPSIS (Technique for Order of Preference by Similarity to Ideal Solution) and VIKOR (Vlsekriterijumska

✉ Raj Kumari
kumari09raj@gmail.com

Mahesh Angira
mahesh_angira@nith.ac.in

[1] Department of Electronics and Communication Engineering, NIT Hamirpur, Hamirpur, H.P. 177005, India

Optimizacija Kompromisno Resenje) [5–7] are the two most common quantitative techniques which provide direct ranking of the materials for various components of the device. There are a variety of RF-MEMS switches categorized based on their switching structure movement and arrangement, contact type and actuation applied. In the present work, a shunt RF-MEMS capacitive switch with an electric actuator is analyzed. The main components of a capacitive MEMS switch determining its performance are the switching structure and dielectric layer. Figure 9 shows the conventional design of a shunt capacitive RF-MEMS switch [8].

A shunt RF-MEMS capacitive switch is formed by a substrate, generally of silicon or glass material, followed by a SiO_2 insulating layer over which a coplanar waveguide (CPW) transmission line is formed. A thin dielectric layer is deposited on the central conductor line of the CPW, which is responsible for the capacitive action of the switch. After a gap of a few micrometers (0.5–5 μm), the structural layer is hung using meanders and anchors made of the same material. This structural layer performs the on and off action when the switch is actuated by applying a biasing voltage between the signal line and structural layer. Normally, in the absence of bias, the switch is in the on position and the signal line allows the signal to be transmitted from one port to another port. When actuation voltage is applied between the RF line and actuating membrane, an electrostatic force develops as a result of capacitive action, and the bridge collapses on the dielectric layer and provides a ground path to the incoming signal. This turns the switch off, as the signal flow through the transmission line is interrupted by the bridge. Here, it is clear from operation of the switch and from the literature that a two-component dielectric layer and switching element is most effective in improving switch performance. In the process of material selection, material indices are the basic building blocks of all the multiple-criteria decision-making (MCDM) techniques. For the dielectric layer, a material with high Young's modulus (YM) ensures a highly rigid structure which can be maintained longer with high-power RF signals, high dielectric permittivity increases the capacitance ratio and thereby improves the RF response, high resistivity results in lower dielectric charging and leakage currents, and high thermal conductivity and a low thermal expansion coefficient (TEC) make the design more robust under high-power operations [9]. Similarly, high YM, thermal conductivity and melting point (MP) and a low TEC value of the material for a structural layer are required to avoid spring softening, self-actuation and thermal runaway problems when the switch deals with high RF power signals. A low value for the ratio of density-to-YM for a structural layer material is desired to keep switching speed high [10]. Therefore, accordingly, these performance parameters are selected as material indices for the dielectric and structural layers to enhance the RF signal power handling and switching speed. With a brief introduction in the first section, this paper is organized as follows: Section 2 discusses the multiple-attribute decision-making (MADM) techniques of material selection and Sect. 3 covers the material database and indices selected for the dielectric and structural layers. Section 4 contains the results of material selection methodologies, and verification of these results is presented through the electromagnetic and electromechanical analysis of the switch. The conclusion is presented in Sect. 5.

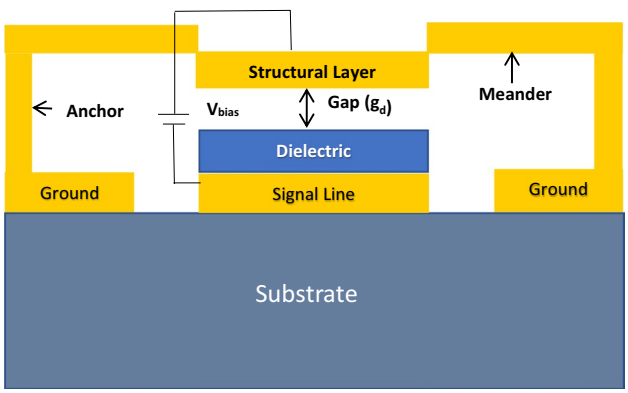

Fig. 1 Shunt capacitive RF-MEMS switch

2 Material selection methods

Material selection is a systematic process that requires complex steps, as material for each component has different properties. MCDM methodologies offer many techniques based on providing a solution by analyzing the selected properties of multiple materials to improve the device performance in the desired manner. In this paper, two very simple and effective quantitative approaches, TOPSIS and VIKOR, are used.

2.1 TOPSIS approach

TOPSIS is a technique that follows a principle in which the material closest to a "positive ideal solution" (A_{PIS}) and farthest from a "negative ideal solution" (A_{NIS}) is kept at position 1 [11]. A list of all possible suitable materials is created, and material indices are selected to form a fundamental decision matrix. Weights are calculated and multiplied with a normalized decision matrix. From this matrix, on the basis of cost and benefit, criteria A_{PIS} and A_{NIS} are determined. Finally, closeness to the positive ideal solution (Ci) is calculated, and based on this, rankings are assigned to the materials. Ci is given as

$$Ci = \frac{Qib}{Qiw} \quad (1)$$

where Q_{ib} is the distance of the criterion from A_{PIS} and Q_{iw} is the distance of the criterion from A_{NIS}. A step-by-step detailed mathematical flow of TOPSIS and Eq. (1) can be found in the literature [5, 6, 9–11].

2.2 The VIKOR method

VIKOR, developed by Serafim Opricovic, is a MADM method for the optimization of material selection using a compromise solution [12]. This technique is more effective as it also considers the impact of the relative distance of an attribute from A_{PIS} and A_{NIS}, and in the end, it provides compromise solution sets. Most of the basic steps in TOPSIS and VIKOR are the same, such as formation of the decision matrix, normalization and weight determination. VIKOR is also known as a modified version of TOPSIS. The process steps of VIKOR have been explained in detail in [5, 6, 9–13]. Ultimately, VIKOR also provides direct ranking of the materials on the basis Qi (quotient) matrix and also calculates the compromise solution if the performance of two attributes is found to be very close to each other. Both methods converge to the same results and thus help to select the best material out of a pool of materials.

3 Material database and indices

A material data set of the 15 most commonly used metals for the structural layer and 10 dielectrics for the dielectric layer were selected from the literature [1, 5–10, 14–16] and are listed in Tables 1 and 2. A state-of-the-art review of materials, MCDM methods and fabrication techniques was reported in [1]. The authors screened out Al, Au and Cu, using the Ashby method for low pull-in voltage and RF losses at high frequencies. These materials were found suitable at high temperature for longer lifetime. The authors also determined that AlN, Al_2O_3 and Si_3N_4 were the preferred choice for fabricating a stiction-free, reliable switch with longer lifetime. The authors in [5] reported TiO_2 as the best dielectric material for low-power applications and AlN for high-power applications on the basis of Ashby, TOPSIS and VIKOR algorithms. Using the same algorithms with criteria of pull-in voltage, RF loss, thermal conductivity and displacement, Au, Al and Cu were described as the best materials in the literature [6, 14]. However, Au is costly and not suitable for commercial applications. Recently [7], Au and Al_2O_3 were found to be the most preferred choice for the bridge and dielectric of a high-performance switch in the frequency range of 50–100 GHz. Furthermore, TiO_2 [9] was observed as the best material out of a list of materials, based on capacitance ratio, leakage current, heat dissipation and thermal expansion. In [10], the authors analyzed different materials using TOPSIS and VIKOR and recommended tungsten and iridium as the most suitable for high-power RF-MEMS switches. The study is focused on a single domain (high power); however, RF-MEMS switches are

Table 1 Structural layer materials with corresponding indices values [1, 6, 7, 10, 16]

Materials	Young's modulus (GPa)	Thermal conductivity (W/m–K)	Thermal expansion coefficient 10^{-6} m/(m K))	Melting point (K)	Density/YM (g cm^3/GPa)
Graphene	1000	165	4.8	3970.15	0.002267
Rh	380	150	8	2237	0.032657895
Fe	211	73	9.71	1811	0.037317536
Au	79	315	14	1336	0.244303797
Cu	117	386	16	1357	0.076581197
Ag	83	407	19	1234	0.126385542
Al	70	237	21	933	0.038571429
W	411	163	4.5	3673	0.046836983
Ir	525	147	6.4	2739	0.042971429
Ru	447	120	9.1	2607	0.027852349
Co	209	69	12	1768	0.042583732
Pt	168	71.6	8.8	3221	0.127678571
Mo	329	143	5	2893.15	0.031246201
Sn	16	35.4	22.5	1042.15	0.16875
Re	463	48	6.2	3459	0.045399568

Table 2 Dielectric layer materials with corresponding index values [1, 5, 7, 9]

Materials	Dielectric permittivity	Resistivity (Ω m)	Thermal conductivity (W/m K)	Thermal expansion coefficient 10^{-6} m/(m K))	Young's modulus (GPa)
Si_3N_4	7	10^{14}	29	3	304
Al_2O_3	8.4	10^{20}	39	7	378
SiO_2	4.1	10^{16}	1.4	2.3	100
HfO_2	25	10^{7}	1.1	6	57
TiO_2	80	10^{10}	11.7	9	230
ZrO_2	22	10^{10}	2.2	12.2	200
AlN	9	10^{11}	140	4.5	330
STO	29	10^{8}	36	3.8	150
ZnO	8.5	10^{13}	60	5.3	40
Ta_2O_5	25	10^{11}	54.4	6.4	186

truly multidisciplinary in nature. Thus, optimum material selection would not reflect the clear-cut selection of materials. Sawant et al. in [15] analyzed different materials using the Ashby technique and selected a contact material for RF-MEMS switches for high-power applications. It has been reported that because of its high elastic modulus, hardness, electrical resistivity and MP, graphene is preferred over Au and rhodium. In the above-discussed papers, materials are selected based on their parameters of interest according to the specific applications. Thus, in the present work, the pool of materials was formed by collecting materials from the literature, and then selection of the best materials was performed and verified under conditions of optimized power and speed.

3.1 Material indices for the structural layer

Five material indices were selected for the structure of the RF-MEMS switch in order to increase its power handling capability and switching speed.

3.1.1 Power handling capability

A RF-MEMS shunt capacitive switch is capable of handling a certain amount of RF power, and if this power is sufficient to provide a voltage equal to or greater than the pull-in voltage of the switch, then a phenomenon called self-actuation occurs. Under this condition, the actuating electrode will establish a connection with the signal line without applying any actuation voltage to the device. In order to omit false actuation, the self-actuation power must be increased to a level such that the RF signal power will not be able to provide sufficient actuation voltage to the switch [17]. Mathematically, input power corresponding to self-actuation can be calculated as

$$P_{\text{input}} = \mathrm{V}_{\text{RF}}^2/\mathrm{Z}_0 \tag{2}$$

$$P_{\text{self}} = \mathrm{V}_{\text{Pull-in}}^2/\mathrm{Z}_0 \tag{3}$$

where P_{input} is input power, P_{self} is self-actuation power, Z_0 is the characteristic impedance of the CPW line and V_{RF} is the root-mean-square value of the RF signal. It is clear from Eqs. (13) and (14) that the self-actuation power should be increased more than the input signal power to minimize the possibility of false actuation. Appropriate switch materials, which may result in higher pull-in voltage and have the thermal conductivity, TEC and MP to withstand high-power operations, can serve the desired objective of enhancing the power handling. Further, this can be done by selecting suitable parameters as material indices in MCDM techniques. These indices are given as follows:

1. Pull-in voltage is a key parameter of the electrostatic switch [18], which is shown in Eq. (3). It depends upon the amount of power a switch can handle. In the case of high power handling, when a high-frequency signal passes through the CPW line, high pull-in voltage is required to avoid false actuation of the switch. Pull-in voltage is a function of material parameters as well as structural parameters as can be seen in the equation given below:

$$v_{\text{p}} = \sqrt{\frac{8\mathrm{kd}^3}{27\varepsilon_{\text{o}}\mathrm{A}}} \tag{4}$$

where k is the spring constant, d is the distance between the metallic structure and micro-actuator, εo is the dielectric constant of free space and A is the area of the plates in the switch. It is clear from the expression that here the parameter under control is k, which is directly proportional to YM. Thus, to determine the impact of

power handling on the structural layer of the switch, the first index of interest, MI_{S1}, is YM denoted by E.

2. Whenever a device has to handle high power, parameters that deal with heat play a very important role. One such parameter is thermal conductivity (λ), which is responsible for the conduction of heat through the material. It ensures a longer device lifetime under the condition of high power. When heat is generated in the structure, it should flow away from the device immediately without affecting its performance [7, 19, 20]. For this purpose, the conduction of heat through the material should be very high. Hence, λ is selected as the second material index, MI_{S2}.
3. Under the impact of high-power signals, many times the thickness of the material changes due to thermal stress. This is not desired for any of the devices. The heating effect due to dc bias causes thermal stress, which may also result in breakdown and poor stability. It has been found in the literature [5, 9, 21] that thermal stress is directly proportional to the coefficient of thermal expansion (α). Thermal stress can be easily reduced by using a material with a very low expansion coefficient [22]. Thus, the third material index, MI_{S3}, is α.
4. For high-power RF signals, the temperature of the metallic membrane increases. To handle this high temperature, the MP of the metallic membrane should be maximal [10]. Thus, MP is selected as the fourth material index, MI_{S4}.

3.1.2 Switching time

Large switching time is again an important issue to be addressed. Because of the involvement of mechanical functionality, RF-MEMS shunt switches lack speed and need further research and development in this area. The switching speed of the MEMS switch depends on various mechanical and electrical parameters, including the natural frequency of the device, spring damping, and pull-in and applied voltage. Therefore, in MCDM techniques, speed is also considered as a criterion, and the corresponding parameter of interest is selected as a material index. Switching time is the total time taken by the structural layer to collapse on the dielectric layer (pull-in time) and return to its initial state (release time). The smaller the value of pull-in and release time, the greater the speed of switching [14, 19, 23]. The pull-in time of the membrane is given as

$$t_{\mathrm{p}} = 3.67\frac{V_{\mathrm{p}}}{V_{\mathrm{s}}.\omega_{\mathrm{o}}} \tag{5}$$

$$t_{\mathrm{p}} = 3.67\frac{V_{\mathrm{p}}}{V_{\mathrm{s}}}\sqrt{\frac{(\mathrm{lwt})\rho}{\mathrm{k}}} \tag{6}$$

where l, w, t are the length, width, and thickness of the bridge, ρ is the density of the membrane material, m is mass of structure, $V_{\mathrm{p}}$and V_{S} are pull-in voltage and switching voltage [14]. The equation to calculate the release time is given as

$$t_{\mathrm{r}} = \frac{1}{4\mathrm{f}} \tag{7}$$

where f is the natural frequency of the switch. Here, switching time is a direct function of the density of the material and is an inverse function of k. Furthermore, k is a direct function of YM. Thus, $\rho/_{\mathrm{E}}$ (ratio of material density to YM) is taken as the fifth material index, MI_{S5}.

3.2 Material indices for the dielectric layer

Material selection for the dielectric layer was performed by considering the criteria of increasing power handling and improving RF response. Five material indices were selected using corresponding performance parameters. These are given as follows:

1. Insertion loss and isolation are the two main parameters responsible for good RF response. These can be expressed in terms of up-state and down-state capacitances of a RF-MEMS capacitive switch, as given below:

   Up-state capacitance (insertion parameters)

$$C_{\mathrm{up}} = \frac{\varepsilon_{\mathrm{o}}\mathrm{A}}{\mathrm{g1} + \frac{\mathrm{td}}{\varepsilon_{\mathrm{r}}}} = \frac{\varepsilon_{\mathrm{o}}\mathrm{A}}{\mathrm{g1}} \tag{8}$$

   where ε_{o} is the dielectric constant for vacuum, ε_{r} is dielectric permittivity, A is the overlap area of the membrane and central conductor, g1 is the gap between the dielectric and bridge, and $\mathrm{t_d}$ is the thickness of the dielectric [24]. The up-state capacitance should be low to obtain low insertion loss. Then the down-state capacitance (isolation parameters) [25]

$$C_d = \frac{\varepsilon_{\mathrm{o}}\varepsilon_{\mathrm{r}}\mathrm{A}}{\mathrm{td}} \tag{9}$$

   A high down-state capacitance is required to obtain high isolation. The overall RF response is defined in terms of the capacitance ratio, which is defined as

$$C_{\mathrm{ratio}} = \frac{\varepsilon_{\mathrm{r}}\mathrm{g}}{\mathrm{td}} \tag{10}$$

   From the above equation it is clear that material with a high dielectric constant is desired to improve the RF response of the switch.

Furthermore, it reduces the hold-down voltage, and thus lower dielectric charging occurs, which also eliminates the sticking problem and increases the reliability of the switch. The hold-down voltage can be given as [7]

$$V_h = \sqrt{\left[\frac{2\mathrm{Ke}}{\varepsilon_o \varepsilon_r A}(g_o - g) + \left(g + \frac{\mathrm{td}}{\varepsilon_r}\right)^2\right]} \tag{11}$$

Based on these facts, ε_r is selected as the first material index, MID1, for the dielectric.

2. In the case of capacitive switches, when actuation voltage is applied, the dielectric material starts charging. Then, as soon as actuation is removed, decay of polarization P(t) occurs. This is given as [5, 26]

$$P(t) = P_p \cdot \exp\left(-\frac{t}{\tau}\right) \tag{12}$$

Equation (12) shows that polarization decay depends upon P_p (polarization in steady state), t (discharging time of capacitor) and τ (relaxation time constant for electrical discharge). Relaxation time constant further depends on dielectric permittivity (ε_r) and resistivity (ρ) of dielectric material. This can be seen from the equation given below:

$$\tau = \varepsilon_r . \rho \tag{13}$$

The decay of polarization should be low in order to minimize dielectric charging and leakage current. However, high resistivity will increase the relaxation time constant, which will further decrease P(t). Thus, a dielectric with very high resistivity (ρ) is desired to reduce the leakage which may cause stiction in switches. In the case of high-power RF signals, there is a greater possibility of stiction due to dielectric charging. Thus, under this condition, high-resistivity materials will lead to good power handling capability. Thus, ρ is selected as the second material index, MID2.

3. High-power RF signals flowing through a device generate heat. In such cases, heat should flow away from the device. For this, the thermal conductivity of the materials used in the device should be high. The higher the thermal conductivity, the greater the heat transfer and lower the effect of temperature, which also enhances the life of the system. Thus, for longer lifetime [24], thermal conductivity (λ) is also considered one of the material indices, MI_{D3}, for the dielectric layer.
4. Again, when a device deals with high power, heating effects cause thermal stress, which may also result in dielectric breakdown and poor stability [5, 7, 15]. Therefore, TEC (α) is taken as an important material index, MI_{D4}, for dielectric material selection.
5. High dielectric rigidity is a parameter required to boost the power handling capability of devices [27]. It is given as

$$G = \frac{E}{2(1+\nu)} \tag{14}$$

where E is YM and ν is Poisson's ratio. A large value of YM gives improved rigidity [28]. Thus, the fifth material index, MI_{D5}, for the dielectric is E.

This work deals with high power handling capability and RF response; thus, all parameters taken as material indices were equally preferred and were assigned equal weights of W = [0.2, 0.2, 0.2, 0.2, 0.2].

4 Material's analysis and verification

4.1 Material analysis of the structural layer via MCDM techniques

After applying all the algorithmic steps discussed above on the decision matrix, a ranking list is generated by TOPSIS as shown below in Table 3, where Q_{ib} is the distance of the criterion from the positive ideal solution, Q_{iw} is the distance of the criterion from the negative ideal solution and C_i is the calculated closeness to the positive ideal solution.

The result shows that graphene followed by iridium and tungsten are ranked at the top position for high-power-handling and high-speed applications. All of these materials have high values of YM, MP and thermal conductivity, and very low values for TEC and switching time (density/YM).

Table 3 TOPSIS result for high power and high speed

Materials	Q_{ib}	Q_{iw}	C_i	Rank
Graphene	0.0614	0.2103	0.7740	1
Rh	0.1132	0.1424	0.5571	6
Fe	0.1450	0.1269	0.4668	9
Au	0.1919	0.0799	0.2941	14
Cu	0.1435	0.1301	0.4755	8
Ag	0.1614	0.1148	0.4156	12
Al	0.1616	0.1217	0.4295	11
W	0.1029	0.1538	0.5993	3
Ir	0.0976	0.1508	0.6071	2
Ru	0.1098	0.1462	0.5711	4
Co	0.1481	0.1205	0.4487	10
Pt	0.1567	0.0990	0.3873	13
Mo	0.1149	0.1493	0.5651	5
Sn	0.2076	0.0405	0.1631	15
Re	0.1187	0.1486	0.5560	7

VIKOR similarly generates a ranking with a set of compromise solutions. These are shown in Table 4, where U_i, R_i and Q_i represent utility, regression and quotient matrices, respectively. VIKOR confirms the result generated from TOPIS by assigning almost the same ranking to the materials, as shown in Table 4. Graphene is ranked at the first position, followed by tungsten and iridium. VIKOR also provides a range of solutions which lie under the minimum distance criterion condition of VIKOR [9–13]. Power handling capability and speed are enhanced at the same time. Both parameters rely on the common property of the materials which is YM, as seen from Eqs. (4) and (6). The three top-ranked materials by TOPSIS and VIKOR are taken into consideration for simulation and validation.

4.2 Material analysis of the dielectric layer via MCDM techniques

A decision matrix $[Xij]_{10\times5}$ which contain ten materials and five material indices, as shown in Table 2, is used for the dielectric layer material selection in both the TOPSIS and VIKOR algorithms. Results obtained from these techniques are shown in Tables 5 and 6.

TOPSIS and VIKOR converge with Al_2O_3 at the first rank, AlN at the second rank and TiO_2 at the third rank. These materials are prioritized over others by assigning high values of permittivity, resistivity, thermal conductivity and YM and a low value of TEC.

Table 4 VIKOR result for high power and high speed

Materials	U_i	R_i	Q_i	Rank
Graphene	0.1336	0.1302	0	1
Rh	0.4425	0.1383	0.2517	5
Fe	0.5692	0.1798	0.6283	10
Au	0.7157	0.2000	0.8653	14
Cu	0.5520	0.1795	0.6154	8
Ag	0.6302	0.1864	0.7140	12
Al	0.6939	0.2000	0.8516	13
W	0.3074	0.1313	0.1168	2
Ir	0.3723	0.1399	0.2192	3
Ru	0.4289	0.1545	0.3589	6
Co	0.6044	0.1819	0.6658	11
Pt	0.5504	0.1805	0.6219	9
Mo	0.3789	0.1421	0.2388	4
Sn	0.9304	0.2000	1.0000	15
Re	0.3906	0.1932	0.6126	7

Table 5 TOPSIS result for dielectric materials with high power handling capability

Materials	Q_{ib}	Q_{iw}	C_i	Rank
Si_3N_4	0.2827	0.1199	0.2978	4
Al_2O_3	0.1944	0.2312	0.5433	1
SiO_2	0.3108	0.0966	0.2372	8
HfO_2	0.2969	0.0739	0.1993	9
TiO_2	0.2605	0.1697	0.3945	3
ZrO_2	0.3024	0.0583	0.1616	10
AlN	0.2498	0.1948	0.4382	2
STO	0.2645	0.1085	0.2909	5
ZnO	0.2836	0.0955	0.2519	7
Ta_2O_5	0.2594	0.1023	0.2828	6

4.3 Material analysis of the dielectric layer via finite element method (FEM) simulation (electromagnetic response)

Material selection was performed using TOPSIS and VIKOR considering different material properties for both the structural and dielectric layers. To validate the tabulated materials, the RF-MEMS shunt capacitive switch was simulated using these materials. Electromagnetic analysis was performed on the Ansys HFSS (high-frequency structure simulator) solver by employing graphite (a thick layer of graphene, > 100 nm) for the structural layer and the first three recommended materials from Table 5 or 6 for the dielectric layer. RF analysis is mainly used to determine the impact of a dielectric material on insertion loss, return loss and isolation. Scattering parameters S_{12} and S_{11} observed during the on-state of the switch are called insertion and return loss, and during the off-state S_{21} results in isolation. Results obtained for insertion loss, return loss and isolation with the recommended dielectric materials are shown in Figs. 1, 2 and 3, respectively. Al_2O_3

Table 6 VIKOR result for dielectric materials with high power handling capability

Materials	U_i	R_i	Q_i	Rank
Si_3N_4	0.6101	0.2000	0.7118	4
Al_2O_3	0.4290	0.1887	0	1
SiO_2	0.7640	0.2000	0.8918	7
HfO_2	0.8096	0.2000	0.9451	9
TiO_2	0.6077	0.2000	0.7089	3
ZrO_2	0.8566	0.2000	1.0000	10
AlN	0.4599	0.2000	0.5361	2
STO	0.6493	0.2000	0.7576	5
ZnO	0.7642	0.2000	0.8920	8
Ta_2O_5	0.6646	0.2000	0.7755	6

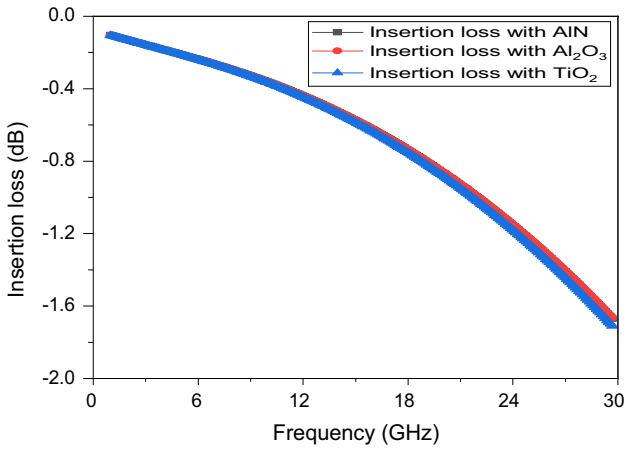

Fig. 2 Insertion loss with the three best dielectric materials

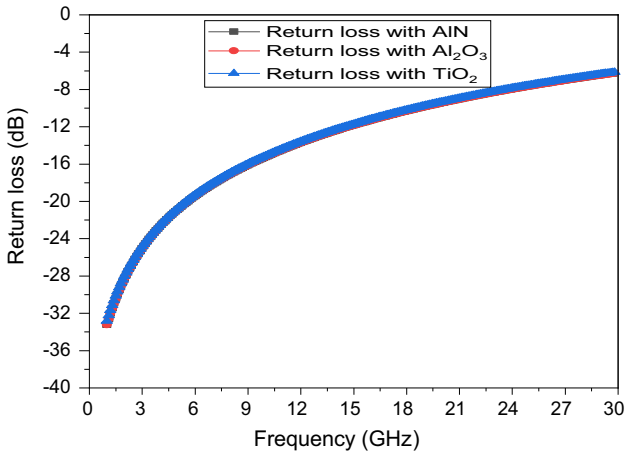

Fig. 3 Return loss with the three best dielectric materials

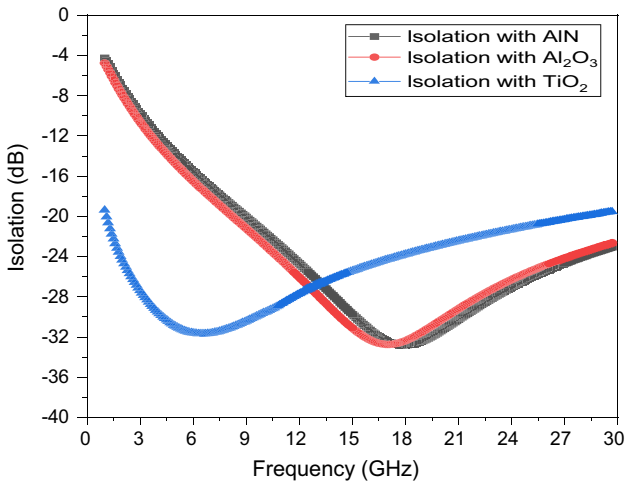

Fig. 4 Isolation of MEMS capacitive switching for the three best dielectric materials

as a dielectric material of the switch provides an isolation peak of −32.74 dB at 17 GHz. When AlN is used in place of Al_2O_3, an isolation peak of −32.53 dB is recorded at 18 GHz, and for TiO_2, peak isolation of −31.69 dB is observed at 6.5 GHz. From the above analysis, it can be concluded that materials selected by TOPSIS and VIKOR result in good and almost identical RF performance. These performance parameters are summarized in Table 7. It is observed that a RF-MEMS switch with dielectric materials Al_2O_3, AlN and TiO_2 shows good response for X and Ku band applications.

4.4 Material analysis of the structural layer via FEM simulation (mechanical response)

In mechanical analysis, the parameter of extreme importance is the spring constant (k). The switch is modeled as a membrane with four supporting arms, and their spring constant can be calculated using Eq. (15) as

$$k = 4\frac{\mathrm{EW}t^3}{\mathrm{L}^3} \tag{15}$$

where E (1000, 525, 411 GPa) is the YM of structural layer materials graphene, Ir and W, respectively, and W (10 μm) is the width of the spring, t (2 μm) is thickness and L (200 μm) is the length of the spring. Calculated spring constant values for graphite, Ir and W are 40, 21 and 16.44 N/m. From the values of spring constant and density of the material, the natural frequency of the device can be calculated using Eq. (16) as

$$f = \frac{1}{2\pi}\sqrt{\frac{k}{m}} \tag{16}$$

where mass of structural part is calculated by multiplying density (∂) with volume (l × w × t). Simulated and mathematically calculated values of natural frequency are shown in Table 8.

Shapes for dominant-mode eigenfrequencies are shown for all three materials in Figs. 4, 5 and 6.

Analysis showed that the graphite switch, which had the highest spring constant value, resonates at the highest frequency, followed by Ir and W. Further, minimizing the switching time is useful. It can be seen from Eq. (7) that the release time is inversely proportional to the natural frequency of the switch. The switch with the highest frequency will result in minimum release time and will reduce the overall switching time. The graphite switch with a frequency of 39.1 kHz resulted in a very small release time of 6.53 μs. The calculated and simulated results for natural frequency converge, as shown in Table 8.

Table 7 Simulated response with top three selected dielectric materials using MCDM methods

Dielectric material	Insertion loss (dB) (8–18 GHz)	Return loss (dB) (8–18 GHz)	Isolation (dB) (8–18 GHz)
$Al2O_3$	−0.29 to −0.73	−17.10 to −10.35	−19.6 to −32.37 −32.74 (17 GHz)
AlN	−0.29 to −0.73	−17.09 to −10.32	−18.61 to −32.53 −32.53 (18 GHz)
TiO_2	−0.29 to −0.75	−16.93 to −10.19	−31.14 to −23.77 −31.68 (6.5 GHz)

Table 8 Natural frequency analysis of the switch with different structural materials

Parameters	Graphene	Iridium	Tungsten
Natural frequency (calculated)	38.3 (kHz)	8.8 (kHz)	8.43 (kHz)
Natural frequency (simulated)	39.1 (kHz)	8.92 (kHz)	8.55 (kHz)
Pull-in time (calculated)	15.2 (μs)	66.3 (μs)	69.2 (μs)
Release time (calculated)	6.53 (μs)	28.4 (μs)	29.7 (μs)

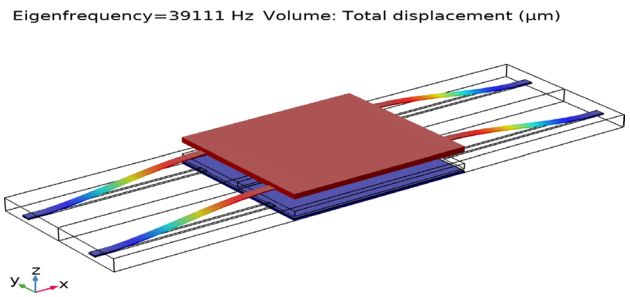

Fig. 5 Graphene switch dominant-mode frequency

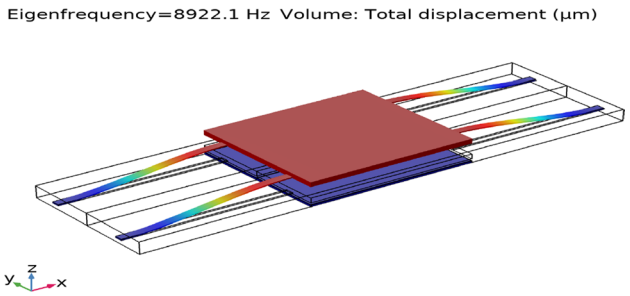

Fig. 6 Iridium switch dominant-mode frequency

4.5 Material analysis of the structural layer via FEM simulation (electromechanical response)

The electromechanical and mechanical response of the switch is analyzed using the COMSOL Multiphysics tool.

Power handling and switching time are the functions of the pull-in voltage and natural frequency of the switch which depend upon YM and density of the structural layer material.

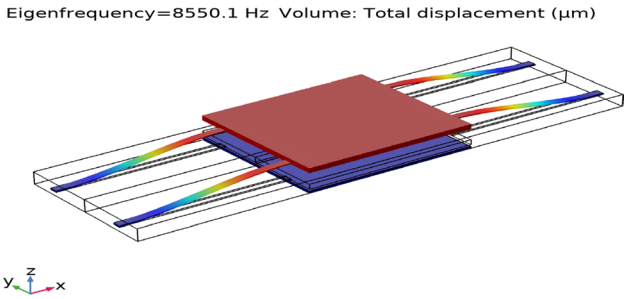

Fig. 7 Tungsten switch dominant-mode frequency

Table 9 Pull-in voltage and spring constant of the switch with different structural materials

Parameters	Graphene	Iridium	Tungsten
Spring constant (calculated)	40 (N/m)	21 (N/m)	16.4 (N/m)
Pull-in voltage (calculated)	38.93 (V)	28.93 (V)	25.59 (V)
Pull-in voltage (simulated)	36.8 (V)	26.2 (V)	23.32 (V)
Self-actuation power (calculated)	27.08 (W)	13.7 (W)	10.87 (W)

A switch structure is simulated using the three best materials from Tables 3 and 4 and Al_2O_3 as a dielectric layer material to validate the results obtained from MCDM techniques. The pull-in voltage for a switch using different materials is calculated using Eq. (4) and tabulated in Table 9 with simulated values. High pull-in voltage omits the possibility of self-actuation by increasing the self-actuation power to a high value such that the RF input signal power will not be able to provide the required amount of power to attain pull-in without applying dc actuation. Self-actuation power for all the materials is calculated using Eq. (3) and is shown in Table 9 along with pull-in voltage and spring constant. Transient self-actuation power variation corresponding to different selected materials is shown in Fig. 7.

Simulated results for pull-in voltage show good agreement with mathematically calculated results. Using values of pull-in voltage, applied voltage, effective mass and spring constant, pull-in time and release time were also calculated for all three materials using Eqs. (6) and (7) and are shown in Table 8. The switching time for the switch was further

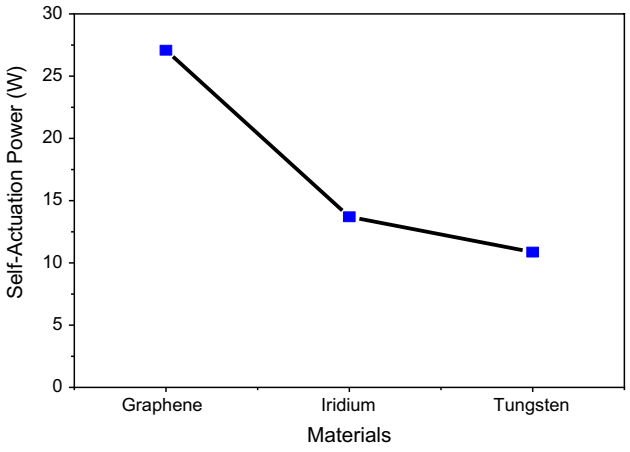

Fig. 8 Transient power variations for graphene, Ir and W

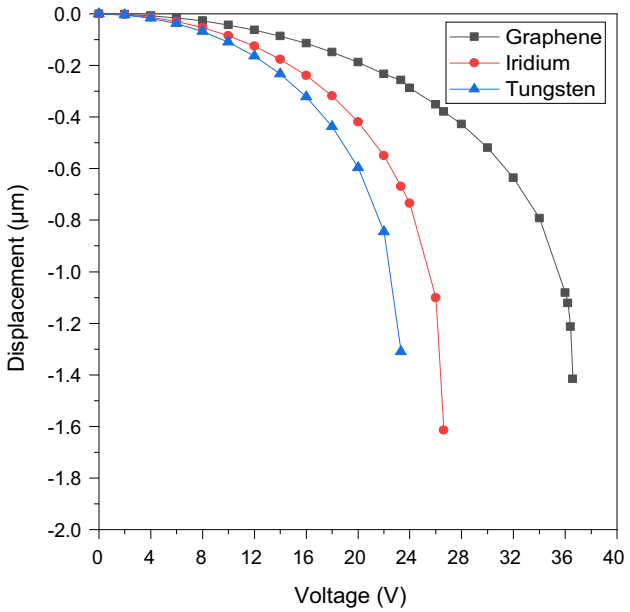

Fig. 9 Pull-in voltage analysis for graphene, Ir and W

approximated using pull-in and release time values. The switch with graphene was observed as the fastest switch with the smallest pull-in (15.2 μs) and release time (6.53 μs) values. Pull-in voltage analysis for the selected best materials is shown in Fig. 9.

4.6 Result verification

In this work, criteria of high power and high speed were set for selecting the optimum material. The material properties showed that YM plays the main role behind high power handling and the ratio of density-to-YM for speed. Graphite has the highest YM value and lowest density-to-YM ratio (Table 1) with respect to other current materials such as W, Ir, Au, Al, and Cu. Graphite also has good thermal properties which are needed at high power. Similarly, among dielectrics, Al_2O_3 has very high YM which keeps it stable at higher temperatures under the impact of high power, and also has the highest resistivity, which helps to avoid stiction (more common at high power). Material analysis for the structural layer in Sect. 4.1 ranked graphene, iridium and tungsten as the top three materials for high-speed and high-power-handling applications. In order to validate the superiority of graphene over other materials, FEM simulation of a standard switch structure was conducted, as shown in Sects. 4.4 and 4.5. As per the simulation outcomes, the resonant frequency of graphite was 38.3 kHz. Since it had the highest resonant frequency among the three materials, it resulted in a minimum pull-in time of 15.2 μs and a release time of 6.53 μs. From Table 8, it is observed that the Ir/Al_2O_3 switch required 81.33% more time (pull-in and release) than graphite/Al_2O_3, and W/Al_2O_3 required 81.98% more time. Furthermore, under electromechanical behavior analysis, the graphite switch showed maximum pull-in voltage of 36.8 V (Table 9); thus it had very high self-actuation power of 27.08 W, followed by Ir and W switches, which validates the results obtained from material selection. From mathematical observations in Table 9, again it is found that the graphite/Al_2O_3 switch can handle 66.40% more power than the Ir/Al_2O_3 switch and 71.39% more than the W/Al_2O_3 switch. Material selection analysis results for the dielectric layer using the MCDM techniques given in Sect. 4.2 was also validated through FEM simulation of the switch shown in Sect. 4.3, with the top three dielectric materials selected in order to ensure good RF response of the device along with the advantage of high power handling capability. The results obtained are tabulated in Table 7 and show that all of the top three selected dielectric materials have good RF response, with the highest insertion (−0.2 to −0.7) and return losses (−17.1 to −10.1) for 8–18 GHz and maximum isolation with Al_2O_3 at −32.74 dB at 17 GHz, followed by −32.53 dB at 18 GHz for AlN and −31.68 dB at 6.5 GHz for TiO_2. The results from material selection analysis are completely validated through FEM simulations, which confirms the suitability of the selected materials for high switching speed, high power handling capability and good RF response within the desired range.

5 Conclusion

Material selection is an important aspect in RF-MEMS switch design, since these are multidomain devices and need to incorporate parameters that apply to multiple domains of power handling, speed and RF losses simultaneously. This work selects optimum material for the bridge and dielectric under conditions of high power and high speed, along with

good RF performance. To the best of the authors' knowledge, this has not been investigated simultaneously for multiple domains in previous studies. Two MCDM methods, TOPSIS and VIKOR, were used with suitable performance parameters for selecting the best materials for the dielectric and structural layers of the switch. Both techniques showed graphene as the most suitable material for the switching structure and Al_2O_3 at the top for the dielectric layer to achieve the desired performance. Furthermore, algorithm results were verified with mathematical expressions and FEM simulations to validate the results of the selected MCDM techniques. It was found from simulation results that with dielectric material Al_2O_3, the switch had insertion loss of 0.2–0.6 dB and return loss of 17.1–10.3 dB for a frequency range of 8–18 GHz. Maximum isolation of 32.74 dB was found at 17 GHz. However, the switch with graphite as a membrane material offered a minimum pull-in time of 15.2 µs and release time of 6.53 µs with natural frequency of 39.1 kHz. The pull-in voltage of 36.8 V was found for the switch, which is sufficiently high to limit false actuation of the switch when dealing with a high-power RF signal. Mathematically calculated and simulated values show good agreement and verify the results obtained from material selection analysis. In the future, selected materials from this work will be used for the implementation of RF-MEMS switches.

Acknowledgements The authors would like to give their sincere thanks to CSIR-Central Electronics Engineering Research Institute, Pilani, for providing software help to complete this work.

Funding No funding has been received from any sources.

Data availability Enquiries about data availability should be directed to the authors.

Declarations

Conflict of interest All authors read and approved the final manuscript and have no conflict of interest.

Ethics approval and consent to participate The research meets all standards with regard to the ethics of experimentation and research integrity. There is no duplicate publication, fraud, plagiarism, or concerns about animal or human experimentation.

References

1. Kurmendra, K.R.: Materials selection approaches and fabrication methods in RF MEMS switches. J. Electron. Mater. **50**, 3149–3168 (2021). https://doi.org/10.1007/s11664-021-08817-8
2. Tilmans, H.A.C., De Raedt, W., Beyne, E.: MEMS for wireless communications: "From RF-MEMS components to RF-MEMS-SiP." J. Micromech. Microeng. (2003). https://doi.org/10.1088/0960-1317/13/4/323
3. Dai, C.L., Chen, J.H.: Low voltage actuated RF micromechanical switches fabricated using CMOS-MEMS technique. Microsyst. Technol. **12**, 1143–1151 (2006). https://doi.org/10.1007/s00542-006-0243-7
4. De Coster, J., Tilmans, H.A.C., Den Toonder, J.M.J., et al.: Empirical and theoretical characterisation of electrostatically driven MEMS structures with stress gradients. Sensors Actuat. A Phys. **123–124**, 555–562 (2005). https://doi.org/10.1016/j.sna.2005.03.075
5. Kumari, R., Angira, M.: Impact of power handling capability on material selection of RF-MEMS switches using MCDM techniques. Proc. 2020 IEEE Int. Symp. Smart Electron. Syst. iSES **2020**, 265–270 (2020). https://doi.org/10.1109/iSES50453.2020.00066
6. Deshmukh, D., Angira, M.: Investigation on switching structure material selection for RF-MEMS shunt capacitive switches using Ashby, TOPSIS and VIKOR. Trans. Electr. Electron. Mater. **20**, 181–188 (2019). https://doi.org/10.1007/s42341-018-00094-3
7. Kurmendra, K.R.: Investigations on beam membrane and dielectric materials using Ashby's methodology and their impact on the performance of a MEMS capacitive switch. Microsyst. Technol. (2021). https://doi.org/10.1007/s00542-021-05220-5
8. Tang, M., Yu, A.B., Liu, A.Q., et al.: High isolation X-band MEMS capacitive switches. Sens. Actuat. A Phys. **120**, 241–248 (2005). https://doi.org/10.1016/j.sna.2004.11.026
9. Patra, P., Angira, M.: Investigation on dielectric material selection for RF-MEMS shunt capacitive switches using Ashby, TOPSIS and VIKOR. trans. Electr. Electron. Mater. **21**, 157–164 (2020). https://doi.org/10.1007/s42341-019-00162-2
10. Angira, M., Deshmukh, D.: Analysis on selection of bridge material for high power RF-MEMS shunt capacitive switches. Trans. Electr. Electron. Mater. **21**, 413–418 (2020). https://doi.org/10.1007/s42341-020-00194-z
11. Manocha, P., Kandpal, K., Goswami, R.: Selection of low dimensional material alternatives to silicon for next generation tunnel field effect transistors. SILICON (2020). https://doi.org/10.1007/s12633-020-00452-y
12. Opricovic, S., Tzeng, G.H.: Compromise solution by MCDM methods: a comparative analysis of VIKOR and TOPSIS. Eur. J. Oper. Res. **156**, 445–455 (2004). https://doi.org/10.1016/S0377-2217(03)00020-1
13. Gangwar, S., Arya, P., Pathak, V.K.: Optimal material selection for ship body based on fabricated zirconium dioxide/ silicon carbide filled aluminium hybrid metal alloy composites using novel fuzzy based preference selection index. SILICON (2020). https://doi.org/10.1007/s12633-020-00600-4
14. Lysenko, I.E., Tkachenko, A.V., Sherova, E.V., Nikitin, A.V.: Analytical approach in the development of RF MEMS switches. Electronics **7**, 1–23 (2018). https://doi.org/10.3390/electronics7120415
15. Sawant, V.B., Mohite, S.S., Cheulkar, L.N.: Comprehensive contact material selection approach for RF MEMS switch. Mater. Today Proc. **5**(4), 10704–10711 (2018). https://doi.org/10.1016/j.matpr.2017.12.352
16. https://www.americanelements.com (2021) Accessed on 9 October 2021.
17. Angira, M., Rangra, K.: Design and investigation of a low insertion loss, broadband, enhanced self and hold down power RF-MEMS switch. Microsyst. Technol. **21**, 1173–1178 (2015). https://doi.org/10.1007/s00542-014-2188-6
18. Sathuluri, M.R., Sasikala, G.: Comprehensive analysis and design of capacitive RF mems switches for reconfigurable microstrip patch antenna. Wirel. Pers. Commun. (2021). https://doi.org/10.1007/s11277-021-09154-z
19. Rao, K.S., Chand, C.G., Sravani, K.G., et al.: Design, modeling and analysis of perforated RF MEMS Capacitive shunt switch. IEEE Access **7**, 74869–74878 (2019). https://doi.org/10.1109/ACCESS.2019.2914260

20. Lucibello, A., Proietti, E., Giacomozzi, F., et al.: RF MEMS switches fabrication by using SU-8 technology. Microsyst. Technol. **19**, 929–936 (2013). https://doi.org/10.1007/s00542-013-1753-8
21. Mahesh, A.: Pathak J (2014) Thin film low voltage RF MEMS shunt capacitive switches using AlN dielectric. Int. Conf. Signal Propag. Comput. Technol. ICSPCT **2014**, 529–532 (2014). https://doi.org/10.1109/ICSPCT.2014.6884955
22. Molinero, D., Aghaei, S., Morris, A.S., Cunningham, S.: Linearity and RF power handling on capacitive RF MEMS switches. IEEE Trans. Microw. Theory Tech. **67**, 4905–4913 (2019). https://doi.org/10.1109/TMTT.2019.2945273
23. Bansal, D., Kumar, P., Kumar, A.: Improvement of RF MEMS devices by spring constant scaling laws. J. Comput. Electron. **20**, 1006–1011 (2021). https://doi.org/10.1007/s10825-021-01657-z
24. Molaei, S., Ganji, B.A.: Design and simulation of a novel RF MEMS shunt capacitive switch with low actuation voltage and high isolation. Microsyst. Technol. **23**, 1907–1912 (2017). https://doi.org/10.1007/s00542-016-2923-2
25. Fernandez-Bolanos Badia, M., Buitrago, E., Ionescu, A.M.: RF MEMS shunt capacitive switches using AlN compared to Si 3N 4 dielectric. J. Microelectromech. Syst. **21**, 1229–1240 (2012). https://doi.org/10.1109/JMEMS.2012.2203101
26. Birmpiliotis, D., Stavrinidis, G., Koutsoureli, M., et al.: On the discharge transport mechanisms through the dielectric film in MEMS capacitive switches. J. Microelectromech. Syst. **29**, 202–213 (2020). https://doi.org/10.1109/JMEMS.2019.2962068
27. Shanthi, G., Srinivasa Rao, K., Girija Sravani, K.: Design and analysis of a RF MEMS shunt switch using U-shaped meanders for low actuation voltage. Microsyst. Technol. **26**, 3783–3791 (2020). https://doi.org/10.1007/s00542-020-04864-z
28. Peroulis, D., Pacheco, S.P., Katehi, L.P.B.: RF MEMS switches with enhanced power-handling capabilities. IEEE Trans. Microw. Theory. Tech. **52**, 59–68 (2004). https://doi.org/10.1109/TMTT.2003.821234